

Supporting Information:

Dioxygen Reactivity of Copper(I)/Manganese(II)-Porphyrin Assemblies: Mechanistic Studies and Cooperative Activation of O₂

Runzi Li, Firoz Shah Tuglak Khan and Shabnam Hematian *

Department of Chemistry and Biochemistry, University of North Carolina at Greensboro, Greensboro, North Carolina 27412

1. UV-vis Spectroscopy

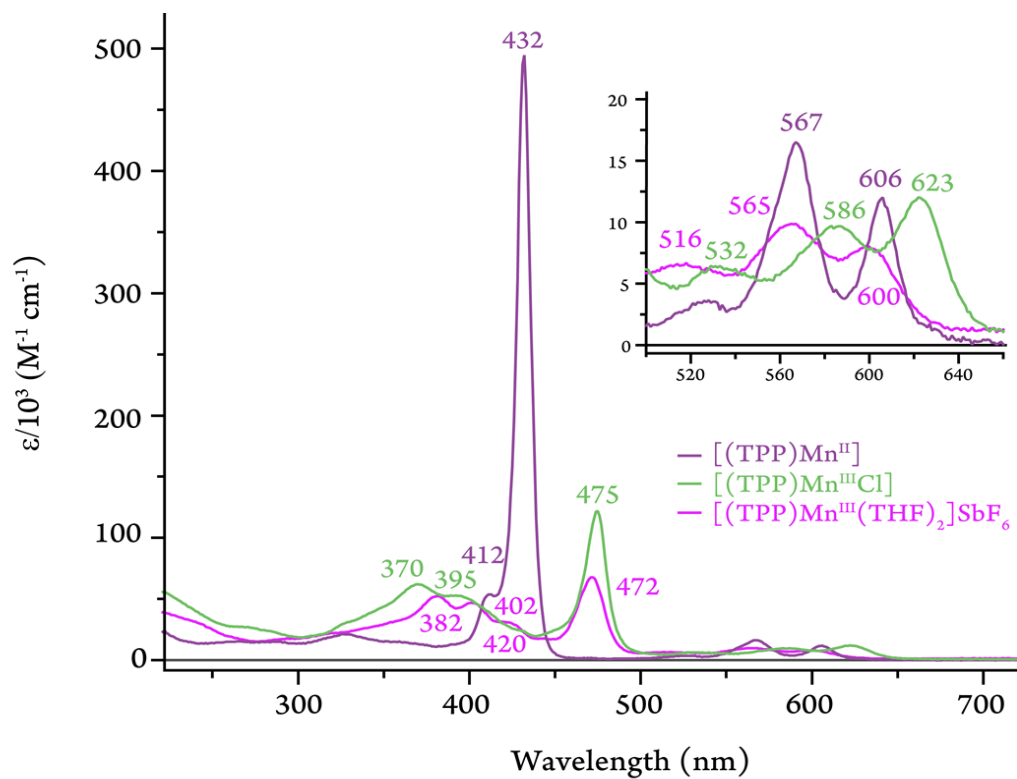


Figure S1. Quantitative electronic spectra of $[(\text{TPP})\text{Mn}^{\text{II}}]$ (purple), $[(\text{TPP})\text{Mn}^{\text{III}}\text{Cl}]$ (green), and $[(\text{TPP})\text{Mn}^{\text{III}}(\text{THF})_2]\text{SbF}_6$ (magenta) in MeTHF at room temperature (RT).

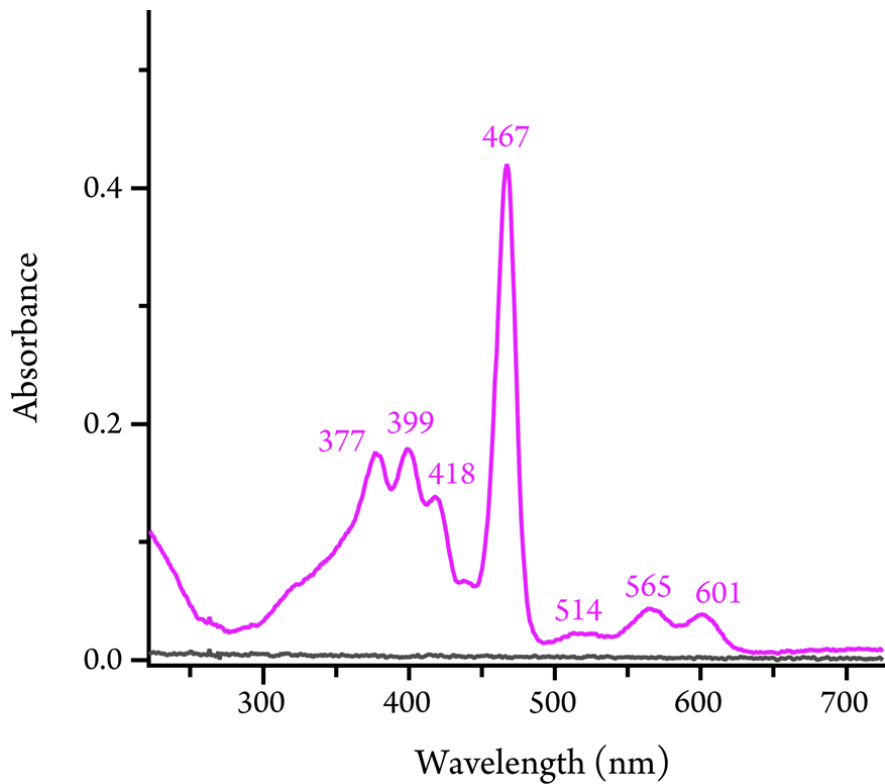


Figure S2. UV-vis spectrum of $[(\text{TPP})\text{Mn}^{\text{III}}(\text{THF})_2]\text{SbF}_6$ in MeTHF at $-110\text{ }^\circ\text{C}$.

2. Crystallographic Studies

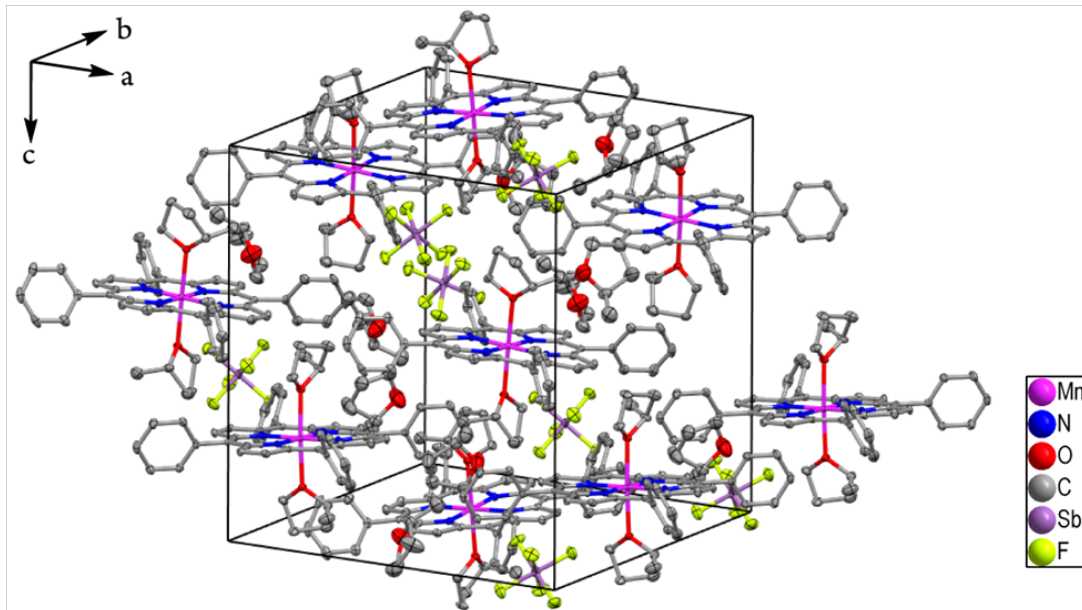


Figure S3. Diagram illustrating the molecular packing of $[(\text{TPP})\text{Mn}^{\text{III}}(\text{MeTHF})_2]\text{SbF}_6 \cdot 2\text{MeTHF}$ at $100(2)\text{ K}$ (hydrogen atoms have been omitted for clarity).

Table S1. Crystallographic Data and Data Collection Parameters for [(TPP)Mn^{III}(MeTHF)₂]SbF₆·2MeTHF.

| | |
|---|---|
| Formula | C ₆₄ H ₆₈ F ₆ MnN ₄ O ₄ Sb |
| T (K) | 100(2) |
| Formula weight | 1247.91 |
| Crystal system | Tetragonal |
| Space group | P 4 ₃ 2 ₁ 2 |
| a, Å | 17.4544(3) |
| b, Å | 17.4544(3) |
| c, Å | 18.6564(7) |
| α, deg | 90 |
| β, deg | 90 |
| γ, deg | 90 |
| V, Å ³ | 5683.8(3) |
| Z | 4 |
| Radiation (λ, Å) | MoKα (0.71073) |
| d _{calcd} , g•cm ⁻³ | 1.458 |
| F(000) | 2568 |
| Crystal size (mm ³) | 0.17 x 0.13 x 0.08 |
| Theta range for data collection | 2.334 to 25.500 ° |
| μ, mm ⁻¹ | 0.770 |
| No of unique data | 5299 |
| Completeness to theta | 99.9% |
| No. of restraints | 0 |
| No. of params. refined | 377 |
| GOF on F ² | 1.015 |
| R1 ^a [I > 2σ(I)] | 0.0359 |
| R1 ^a (all data) | 0.0494 |
| wR2 ^b (all data) | 0.0859 |
| Largest diff. peak and hole | 0.736 and -0.325 e.Å ⁻³ |

$$^a R1 = \frac{\sum |F_o| - |F_c|}{\sum |F_o|}, \quad ^b wR2 = \sqrt{\frac{\sum [w(F_o^2 - F_c^2)^2]}{\sum [w(F_o^2)]^2]}}$$

Table S2. Selected structural parameters for six coordinated Mn(III) porphyrin complexes having bis-axial oxygen ligation in charge neutral ligands.

| Complex | Mn–O _{ax} (Å) ^a | Mn–N _{por} (Å) ^a | Reference |
|---|-------------------------------------|--------------------------------------|-----------|
| [(TPP)Mn ^{III} (MeTHF) ₂]SbF ₆ | 2.272(3) | 2.008(2) | This work |
| [(TPP)Mn ^{III} (CH ₃ OH) ₂]ClO ₄ | 2.261(2) | 2.006(2) | [1] |
| [(TPP)Mn ^{III} (<i>N,N</i> -dimethylformamide) ₂]ClO ₄ | 2.217(4) | 2.010(5) | [2] |
| [(TPP)Mn ^{III} (2,6-lutidine <i>N</i> -oxide) ₂]ClO ₄ | 2.264(4) | 1.996(4) | [3] |
| [(TPP)Mn ^{III} (H ₂ O) ₂]ClO ₄ | 2.271(2) | 2.004(2) | [4] |
| [(TPP)Mn ^{III} (CH ₃ OH) ₂]SbCl ₆ | 2.283(5) | 2.002(2) | [5] |
| [(TPP)Mn ^{III} (ONC ₆ H ₄ NEt ₂) ₂]SbF ₆ | 2.211(4) | 2.016 (4) | [6] |
| [(DHPP ^b)Mn ^{III} (THF) ₂]Cl | 2.320(2) | 2.004(2) | [7] |
| [(TPP)Mn ^{III} (THF) ₂][(Pc ^c)Co ^{III} (L ^d) ₂] | 2.307(2) | 2.007(2) | [8] |

^aAverage value; ^bDHPP corresponds to 5,10,15,20-Tetrakis(3',5'-dihydroxyphenyl)porphyrinato; ^cPc corresponds to phthalocyaninato; ^dL corresponds to 1-phenyl-1H-tetrazole-5-thiolate.

3. NMR Spectroscopy

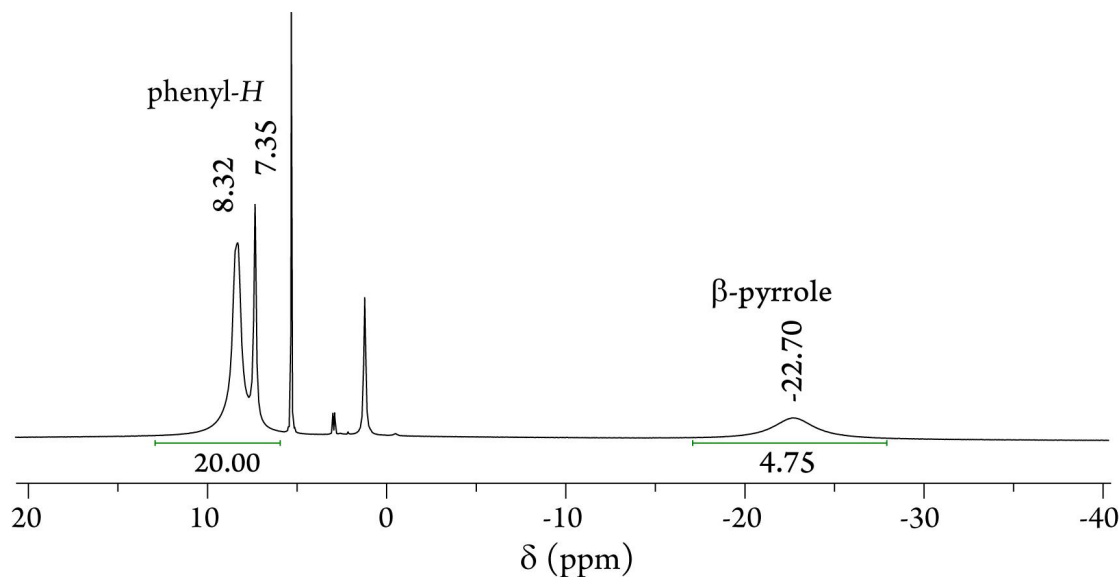


Figure S4. ¹H-NMR spectrum of [(TPP)Mn^{III}Cl] recorded in CD₂Cl₂ at room temperature.

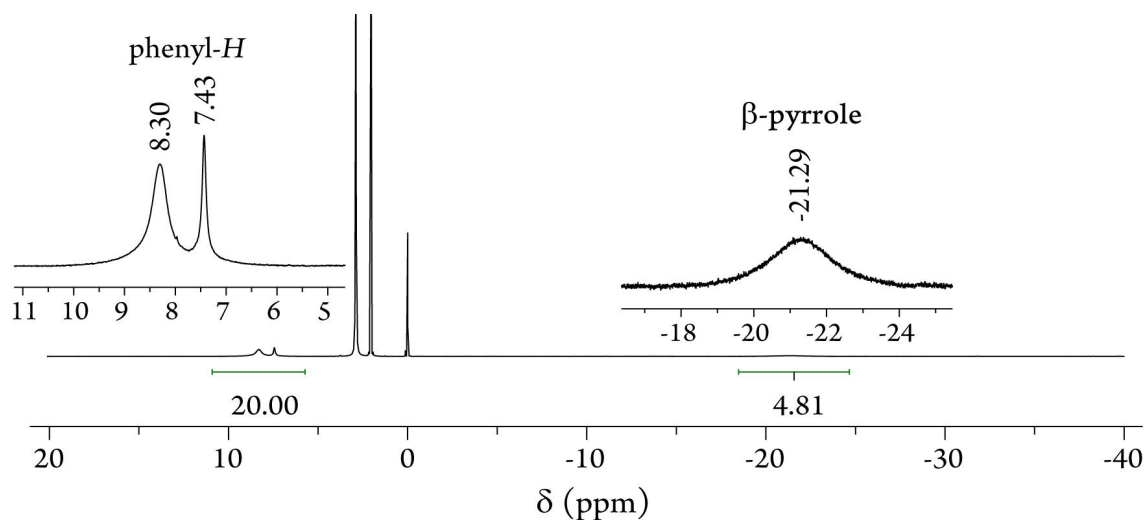


Figure S5. ¹H-NMR spectrum of [(TPP)Mn^{III}Cl] recorded in acetone-*d*₆ at room temperature.

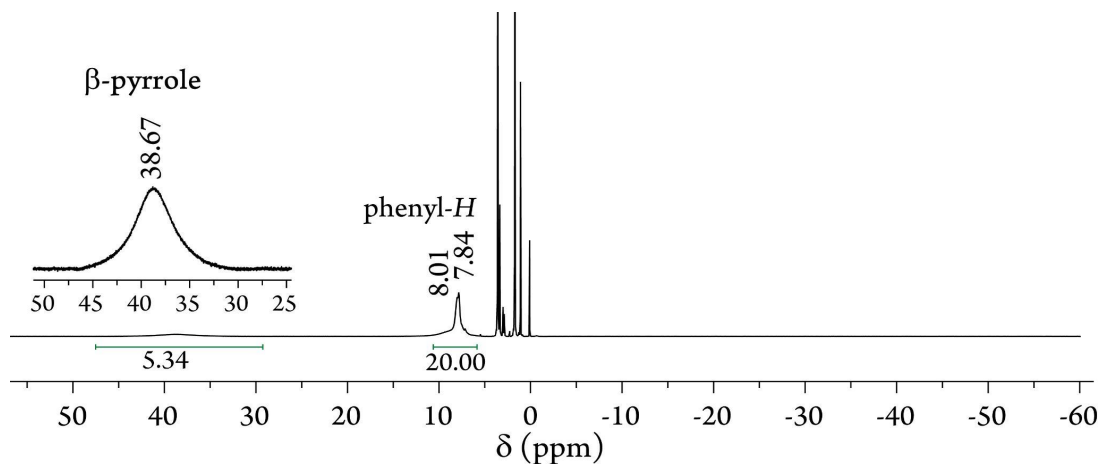


Figure S6. ¹H-NMR spectrum of [(TPP)Mn^{II}] recorded in THF-*d*₈ at room temperature.

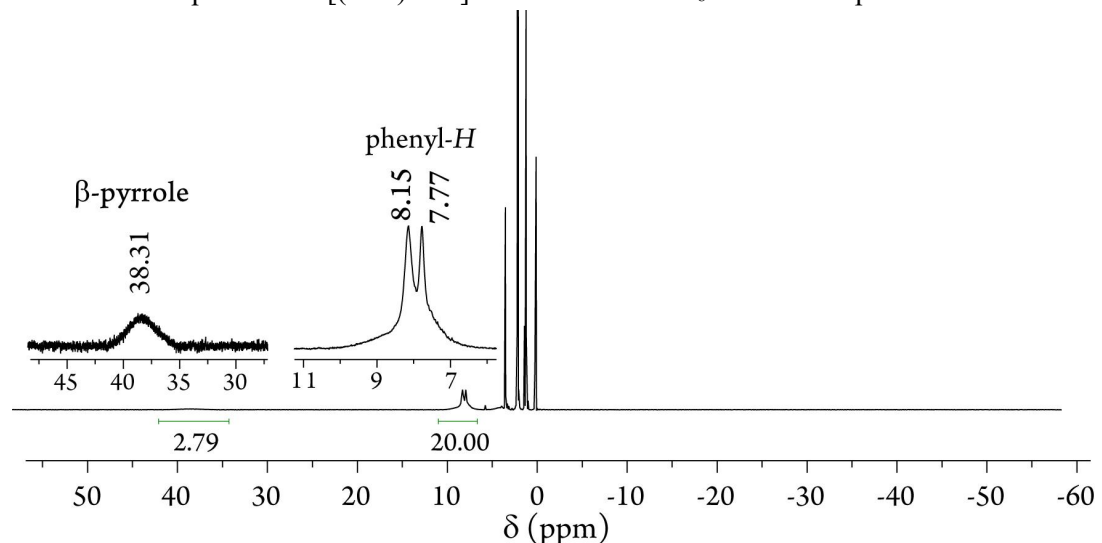
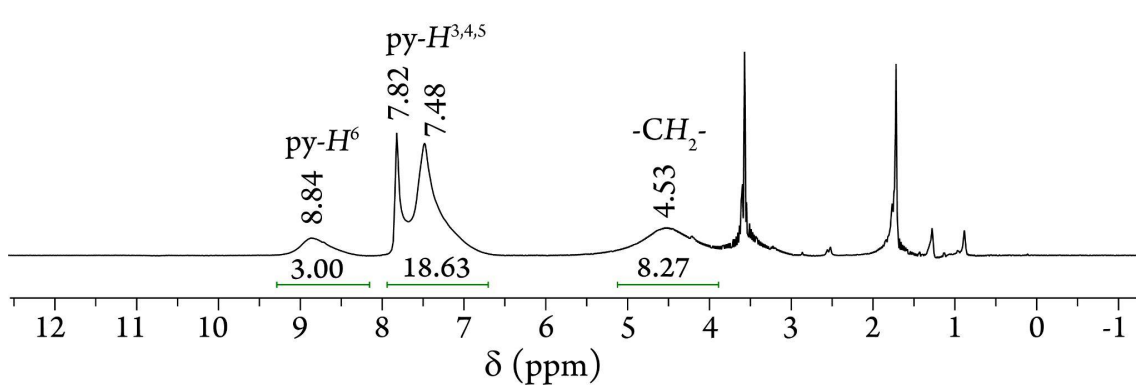
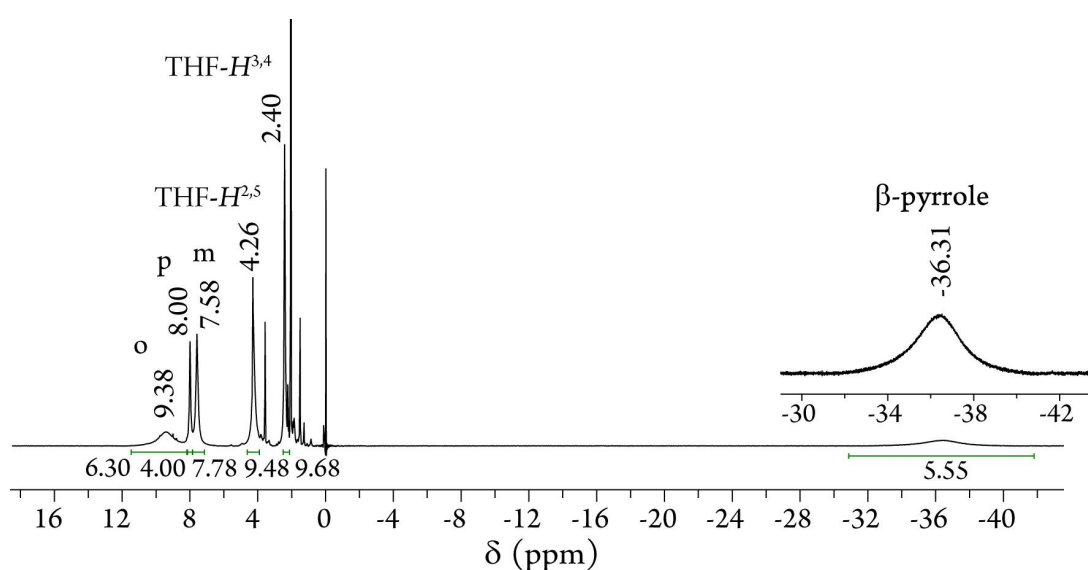
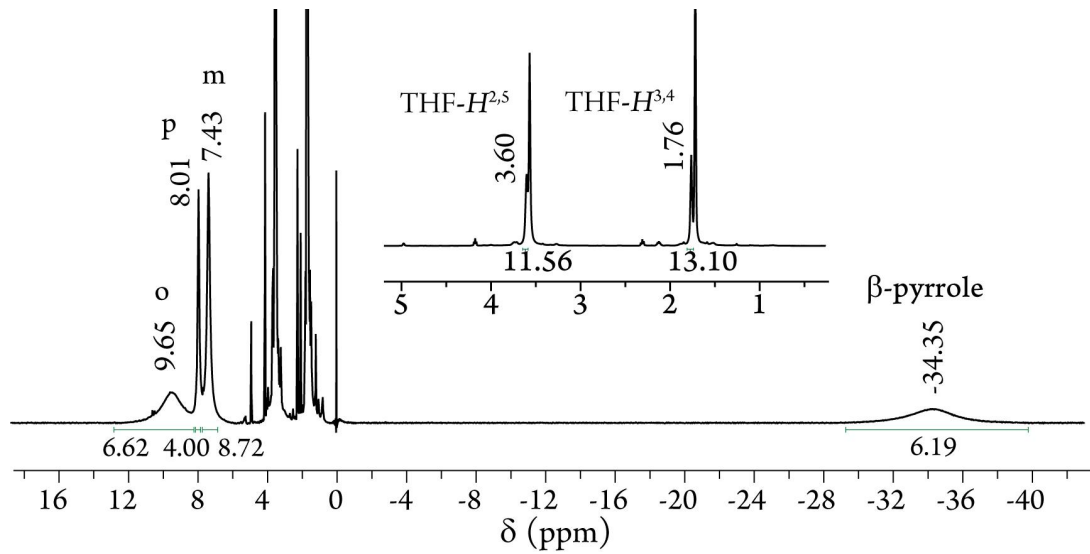


Figure S7. ¹H-NMR spectrum of [(TPP)Mn^{II}] recorded in acetone-*d*₆ at room temperature.



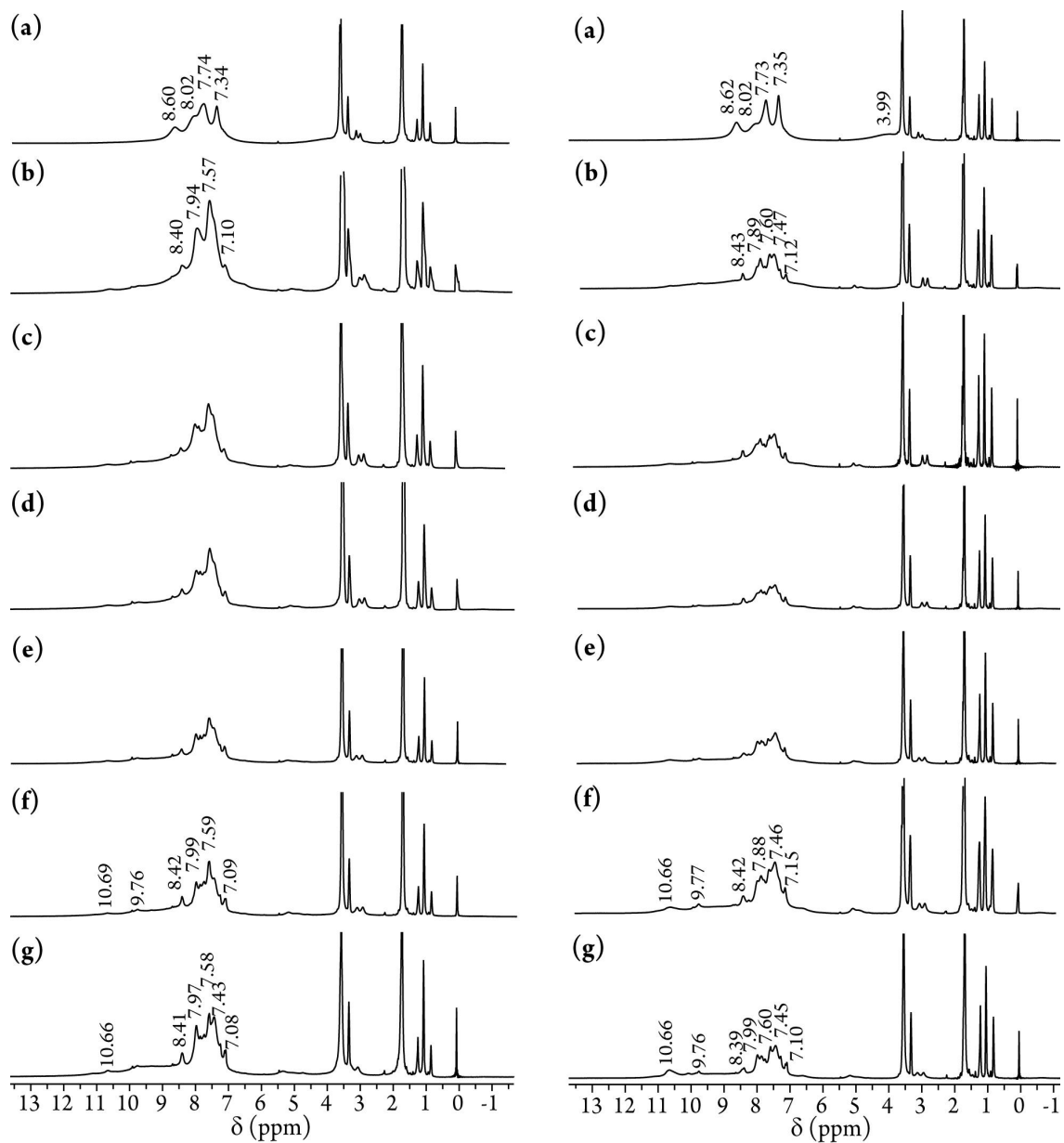


Figure S11. ^1H -NMR spectra (selected portions only) (THF- d_8 , room temperature) of the oxygenation reaction of a 1:1 mixture, *Left*, and 1:2 mixture, *Right*, of $[(\text{TPP})\text{Mn}^{\text{II}}]$ and $[(\text{tmpa})\text{Cu}^{\text{I}}(\text{MeCN})][\text{B}(\text{C}_6\text{F}_5)_4]$ at different time intervals: (a) 0 min, (b) 1 min, (c) 15 min, (d) 1 h 30 min, (e) 4 h 30 min, (f) 6 h, and (g) 18 h.

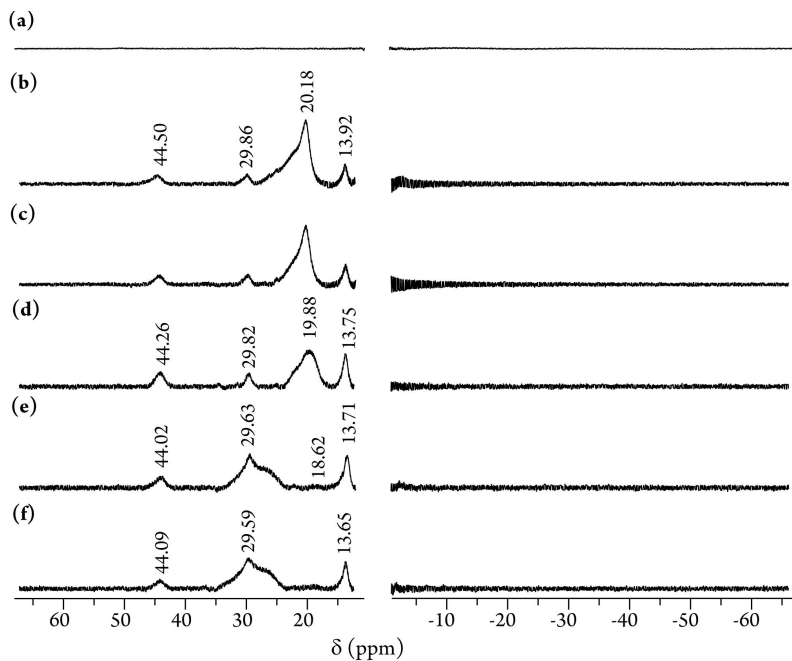


Figure S12. ^1H -NMR spectra (selected portions only) ($\text{THF}-d_8$, room temperature) of the oxygenation reaction of $[(\text{tmpa})\text{Cu}^{\text{l}}(\text{MeCN})][\text{B}(\text{C}_6\text{F}_5)_4]$ at (a) 0 min, (b) 1 min, (c) 15 min, (d) 1 h 30 min, (e) 4 h 30 min, and (f) 6 h.

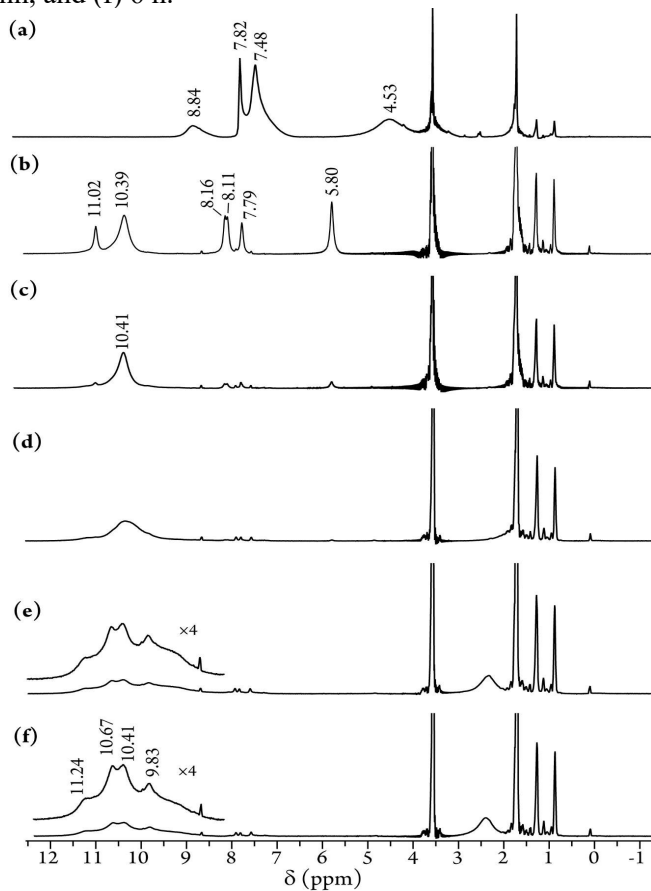


Figure S13. ^1H -NMR spectra (selected portions only) ($\text{THF}-d_8$, room temperature) of the oxygenation reaction of $[(\text{tmpa})\text{Cu}^{\text{l}}(\text{MeCN})][\text{B}(\text{C}_6\text{F}_5)_4]$ at (a) 0 min, (b) 1 min, (c) 15 min, (d) 1 h 30 min, (e) 4 h 30 min, and (f) 6 h.

4. Infrared (IR) Spectroscopy

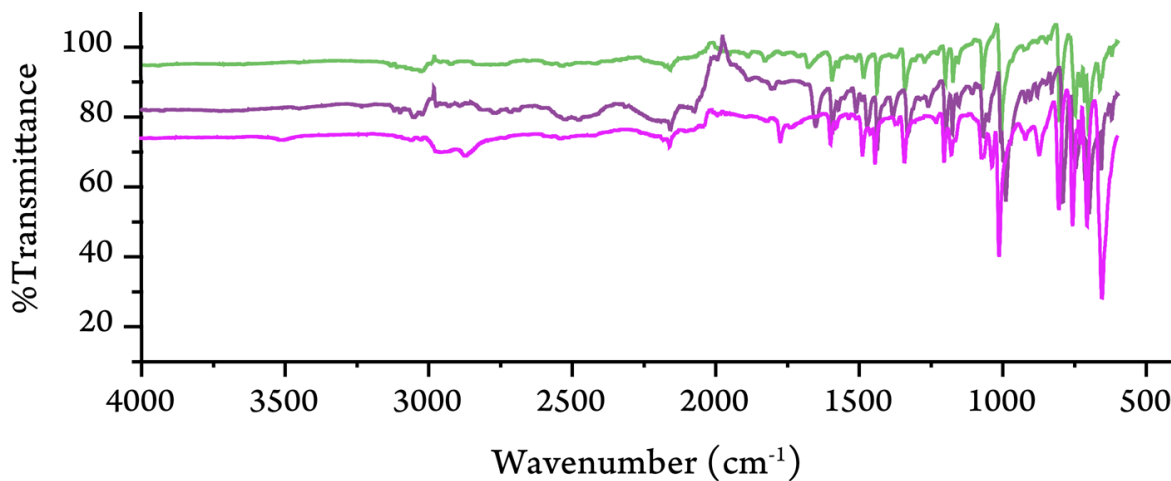


Figure S14. IR spectra of $[(\text{TPP})\text{Mn}^{\text{II}}]$ (purple), $[(\text{TPP})\text{Mn}^{\text{III}}\text{Cl}]$ (green), and $[(\text{TPP})\text{Mn}^{\text{III}}(\text{THF})_2]\text{SbF}_6$ (magenta).

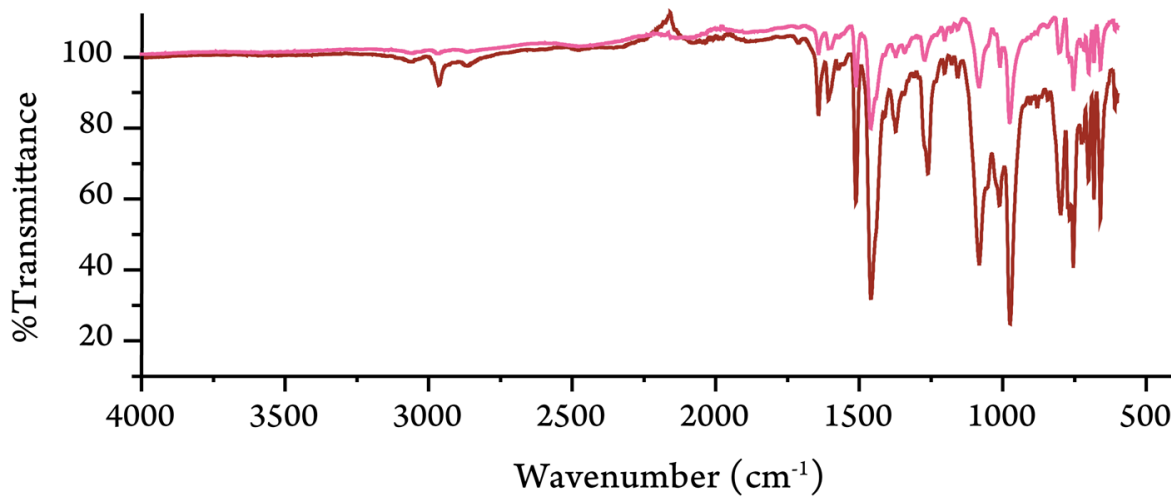


Figure S15. IR spectra of oxygenation products of $[(\text{TPP})\text{Mn}^{\text{II}}]$ with: 1 eq. of $[(\text{tmpa})\text{Cu}^{\text{I}}(\text{MeCN})][\text{B}(\text{C}_6\text{F}_5)_4]$ (pink) or 2 eq. of $[(\text{tmpa})\text{Cu}^{\text{I}}(\text{MeCN})][\text{B}(\text{C}_6\text{F}_5)_4]$ (maroon).

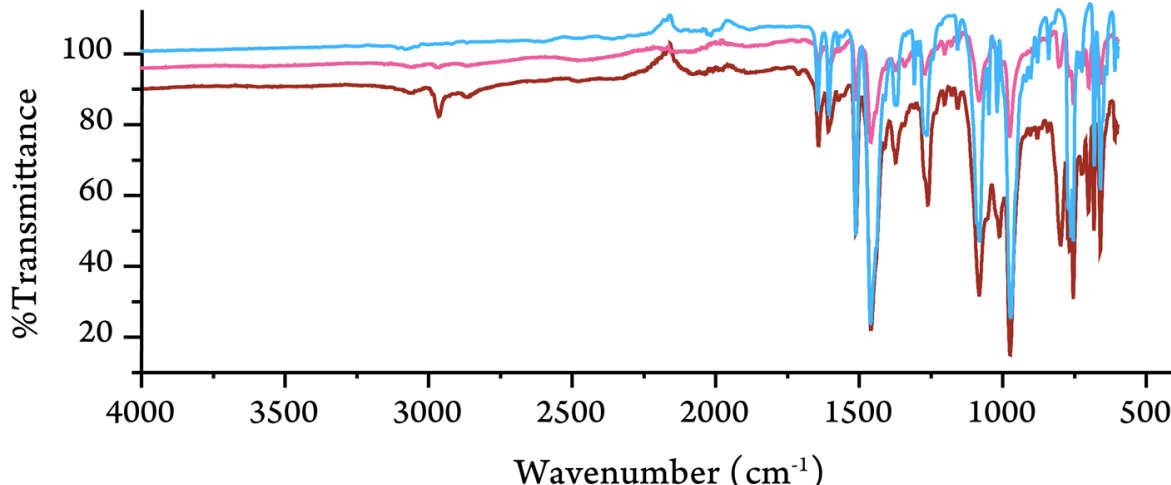


Figure S16. IR spectra of $[(\text{tmpa})\text{Cu}^{\text{II}}\text{Cl}][\text{B}(\text{C}_6\text{F}_5)_4]$ (blue) and the oxygenation products of $[(\text{TPP})\text{Mn}^{\text{II}}]$ with: 1 eq. of $[(\text{tmpa})\text{Cu}^{\text{I}}(\text{MeCN})][\text{B}(\text{C}_6\text{F}_5)_4]$ (pink) or 2 eq. of $[(\text{tmpa})\text{Cu}^{\text{I}}(\text{MeCN})][\text{B}(\text{C}_6\text{F}_5)_4]$ (maroon).

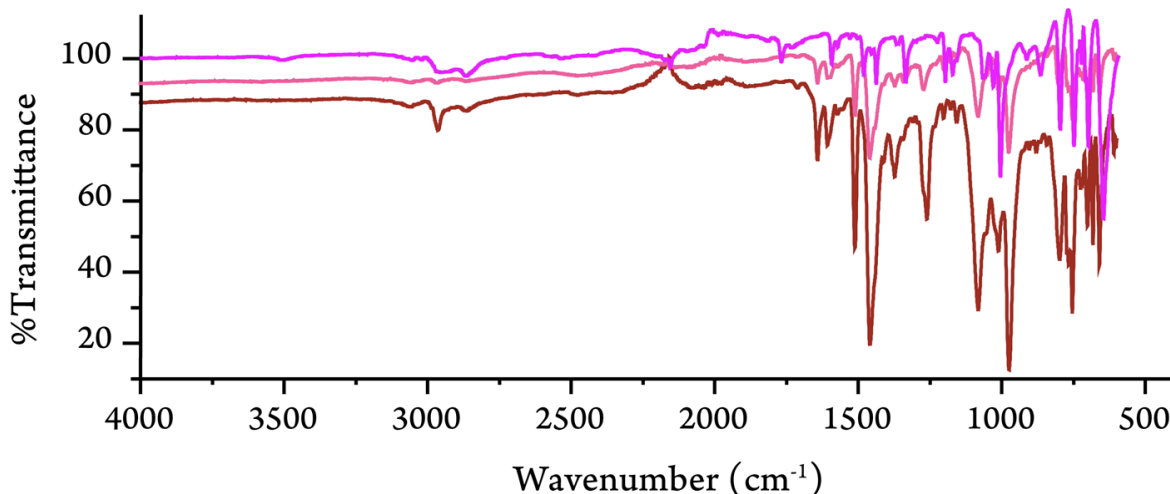


Figure S17. IR spectra of $[(\text{TPP})\text{Mn}^{\text{III}}(\text{THF})_2]\text{SbF}_6$ (magenta) and the oxygenation products of $[(\text{TPP})\text{Mn}^{\text{II}}]$ with: 1 eq. of $[(\text{tmpa})\text{Cu}^{\text{I}}(\text{MeCN})][\text{B}(\text{C}_6\text{F}_5)_4]$ (pink) or 2 eq. of $[(\text{tmpa})\text{Cu}^{\text{I}}(\text{MeCN})][\text{B}(\text{C}_6\text{F}_5)_4]$ (maroon).

Table S3. Metal-sensitive IR bands (cm^{-1}) of TPP manganese complexes.*

| TPP | $[(\text{TPP})\text{Mn}^{\text{II}}]$ | $[(\text{TPP})\text{Mn}^{\text{III}}\text{Cl}]$ | $[(\text{TPP})\text{Mn}^{\text{III}}(\text{THF})_2]\text{SbF}_6$ | 1:1 eq. Product | 1:2 eq. Product |
|------|---------------------------------------|---|--|-----------------|-----------------|
| 1596 | 1594 | 1595 | 1598 | 1598 | 1598 |
| 1491 | 1473 | 1486 | 1487 | 1487 (sh) | 1487 (sh) |
| 1350 | 1333 | 1341 | 1340 | 1342 | 1342 |
| 1003 | 990 | 1006 | 1010 | 1010 | 1011 |
| 966 | 972 | 966 (sh) | 971 | (very broad) | (very broad) |

* TPP data from Ref. [9]. TPP: Tetraphenylporphyrin. “1:1 eq. Product” and “1:2 eq. Product” refer to the oxygenation products of 1:1 and 1:2 eq. mixtures of $[(\text{TPP})\text{Mn}^{\text{II}}]$ and $[(\text{tmpa})\text{Cu}^{\text{I}}(\text{MeCN})][\text{B}(\text{C}_6\text{F}_5)_4]$, respectively.

References

1. Hatano, K.; Anzai, K.; Iitaka, Y. The crystal and molecular structure of bis(methanol)- $\alpha,\beta,\gamma,\delta$ -tetraphenylporphinatomanganese(III) perchlorate-methanol. A molecular structure relevant to the intermediate-spin six coordinate iron(III) porphyrin. *Bull. Chem. Soc. Jpn.* **1983**, *56*, 422-427, 10.1246/bcsj.56.422.
2. Hill, C.L.; Williamson, M.M. Structural and electronic properties of six-coordinate manganese(III) porphyrin cations. Crystal and molecular structure of bis(N,N-dimethylformamide)(tetraphenylporphinato)manganese(III) perchlorate, $[\text{Mn}^{\text{III}} \text{TPP}(\text{DMF})_2]^+\text{ClO}_4^-$. *Inorg. Chem.* **1985**, *24*, 2836-2841, 10.1021/ic00212a027.
3. Hill, C.L.; Williamson, M.W. Electronic and structural properties of a reactive metalloporphyrin with N-oxide axial ligands. Crystal and molecular structure of bis(2,6-lutidine N-oxide)(tetraphenylporphinato)manganese(III) perchlorate. *Inorg. Chem.* **1985**, *24*, 3024-3030, 10.1021/ic00213a031.
4. Williamson, M.N.; Hill, C.L. Molecular stereochemistry of aquamanganese(III) porphyrins. Demonstrable effect of π -arene-porphyrin interaction in the metal coordination environment in the metalloporphyrin. *Inorg. Chem.* **1987**, *26*, 4155-4160, 10.1021/ic00272a005.

5. Scheidt, W.R.; Pearson, W.B.; Gosal, N. Structure of bis-(methanol)(meso-tetra-phenylporphinato)manganese(III) hexa-chloro-antimonate bis-(tetra-chloro-ethane) solvate. *Acta Cryst.* **1988**, *C44*, 927–929, 10.1107/S0108270187012411.
6. Fox, S.J.; Chen, L.; Khan, M.A.; Richter-Addo, G.B. Nitrosoarene complexes of manganese porphyrins. *Inorg. Chem.* **1997**, *36*, 6465–6467, 10.1021/ic970836b.
7. Bhyrappa, P.; Wilson, S.R.; Suslick, K.S. Hydrogen-bonded porphyrinic solids: Supramolecular networks of octahydroxy porphyrins. *J. Am. Chem. Soc.* **1997**, *119*, 8492–8502, 10.1021/ja971093w.
8. Tong, S.-l.; Zhang, J.; Yan, Y.; Hu, S.; Yu, J.; Yu, L. Self-assembled supramolecular architecture with alternating porphyrin and phthalocyanine, bonded by hydrogen bonding and π – π stacking. *Solid State Sci.* **2011**, *13*, 1967–1971, 10.1016/j.solidstatesciences.2011.08.026.
9. Kincaid, J.; Nakamoto, K. Vibrational spectra of transition metal complexes of tetraphenylporphine. *J. Inorg. Nucl. Chem.* **1975**, *37*, 85–89, 10.1016/0022-1902(75)80130-8.